Photoinduced transformation of waste-derived soluble bio-based substances

(Article begins on next page)

20 November 2023

Photoinduced transformation of waste-derived soluble bio-based substances

P. Avetta [a], S. Berto [a], A. Bianco Prevot [a] *, M. Minella [a], E. Montoneri [b], D. Persico [a], D. Vione [a], M. C. Gonzalez [c], D. O. Mártire [c], L. Carlos [d], A. Arques [e]

[a] University of Torino, Department of Chemistry, Via P. Giuria 7, 10125 Torino (Italy).

[b] Via XXIV Maggio 25, 37126 Verona, Italy.

[c] Instituto de Investigaciones Fisicoquímicas Teóricas y Aplicadas (INIFTA), CCT-La Plata-CONICET, Universidad Nacional de La Plata, Diag 113 y 64, La Plata, Argentina.

[d] Instituto de Investigación y Desarrollo en Ingeniería de Procesos, Biotecnología y Energías alternativas, PROBIEN (CONICET-UNCo), Buenos Aires 1400, Neuquén, Argentina.

[e] Grupo de Procesos de Oxidación Avanzada, Dpto de Ingeniería Textil y Papelera, Universitat Politècnica de València. Plaza Ferrándiz y Carbonell s/n, Alcoy, Spain.

*To whom correspondence should be addressed
Tel. +39 0116705292
Fax +39 0116707615
e-mail alessandra.biancoprevot@unito.it

Keywords

Phototransformation processes, biowaste, soluble bio-based substances, fluorescence matrix, spectral slope

Abstract

Waste-derived, soluble bio-based substances (SBO), are effective low-cost photosensitizers that could find application in pollutant photodegradation. For this reason, it is important to understand if and to what extent irradiation could modify their properties. The exposure of SBO to simulated sunlight induced important spectral and structural modifications. Both the whole material and its acid-soluble fraction were characterized, highlighting several properties in common with humic and fulvic substances, including absorption spectra, specific absorbance and fluorescence behavior. The latter was described with a three-component model using PARAFAC analysis. Irradiation induced SBO photobleaching, but the absorbance of the acid-soluble fraction increased with irradiation. This finding suggests a progressive photochemical solubilization of SBO, which is confirmed by the increase of the carboxylic groups. In addition to absorbance, the fluorescence of whole SBO was

1

also decreased by irradiation, thereby suggesting that both chromophores and fluorophores were photodegraded. The increasingly hydrophilic character given to SBO by irradiation also accounted for the photoinduced decrease of the surfactant properties of the material.

1. Introduction

Among the general concern about waste collection, recycling, treatment and/or disposal, the development of processes to valorize the organic fraction of waste, either urban or from agriculture, is a challenge that is increasingly attracting research groups from all over the world. Up to a few years ago, the main goal has been to obtain energy out of organic wastes, by direct combustion or through their anaerobic fermentation for biogas production. However, none of these two approaches is self-sustainable in term of either costs or energy balance. An alternative direction that is gaining increasing interest is the development of the so-called biorefinery. Here the integration of different approaches and processes for organic waste treatment should optimize their exploitation, in terms of both energy recovery and bio-fuel production. Moreover, it includes the separation of value-added chemicals to be released on the market for specific applications. For instance, from the soluble fraction of organic urban waste it has been possible to separate substances showing surfactant behavior and having promising performances in agriculture, animal husbandry, textile dyeing, material synthesis, and pollutant photodegradation [1,2].

Organic pollutant photodegradation has been studied because of the observed similarity, in terms of both structure and physical-chemical properties, between the waste-derived soluble bio-based substances (SBO) and the natural organic matter present in soils or as Dissolved or Particulate Organic Matter (DOM or POM) in natural waters, specifically the humic acid fraction. Therefore, SBO have also been presented as "humic acid-like" substances [3]. Many contributions can be found in the literature about DOM photoactivity in natural waters and on its important role in the photoassisted transformation of xenobiotics [4-6]. Based on these premises, SBO have been studied for their capability to promote the photodegradation of various pollutants, with several encouraging results [3,7-8]. In these studies it has also been evidenced a slow but progressive transformation of SBO upon irradiation under simulated sunlight [9].

SBO can be isolated from waste either in their acidic form, or as potassium /sodium salts. In the former case, the "humic-like" SBO can be separated from the "fulvic-like" fraction on the basis of their different solubility at pH < 2. In the latter case, isolation of the SBO "humic like" fraction is attained through an ultrafiltration step, exploiting the different size of the "humic like" and "fulvic like" components of SBO [1,10]. At least theoretically, the substances obtained in the two cases

2

should only differ in their acidic properties. However, a peculiar behavior has been observed with ultrafiltration-derived SBO, because they do not undergo complete precipitation when the solution pH is lowered to about 1.5. The brownish color of the aqueous phase suggests that some dissolved organic compounds were still present in solution. This fraction of SBO (hereinafter SBO$_{sol}$), which is soluble at pH < 1.5, deserves attention because of its stronger photosensitizing effect compared to SBO itself, shown in preliminary results.

The present research aims at giving more insight into SBO photodegradation processes. To better understand SBO photoageing, different analytical approaches have been chosen to assess the photoinduced SBO transformation in terms of structure, surfactant properties, aggregate dimensions and degree of mineralization. Attention was also devoted to the acidic functions present in the SBO structure, which could form bonds with metal ions, e.g. iron. Indeed, SBO are promising compounds to perform photo-Fenton processes under mild conditions, because they can maintain Fe(III) in solution at pH values above 4.5-5 [11]. In contrast, the classical photo-Fenton reaction requires acidic conditions where Fe(III) does not precipitate as hydroxide and the $^{\bullet}$OH radical production via the Fenton process reaches its maximum efficiency.

2. Experimental

2.1 Reagents

NaOH, KOH, HCl, HClO$_4$, H$_2$O$_2$ and tetraethylammonium chloride were purchased from Aldrich and used as received. All aqueous solutions were prepared with ultra-pure water, obtained from a Millipore Milli-Q^{TM} system.

Among different available SBO, the so-called CVT230 was chosen as a model because most of the published papers about the photosensitized degradation of pollutants with SBO dealt with this material. CVT230 has been isolated from urban bio-wastes (UBW) sampled from the process lines of ACEA Pinerolese waste treatment plant in Pinerolo, Italy. The UBW was obtained in the compost production section, from urban public park trimming and home gardening residues aged for 230 days. It was further processed in a pilot plant located in Rivarolo Canavese, Italy [2], by means of an electrically heated and mechanically stirred 500 L reactor, a 102 cm long × 10.1 cm diameter polysulfone ultrafiltration (UF) membrane with 5 kD molecular weight cut-off (supplied by Idea Engineering s.r.l.), and a forced ventilation drying oven. According to the operating experimental conditions, UBW were digested for 4 h at 60 °C, pH 13 and 4/1 V/w water/solid UBW ratio. The resulting heterogeneous mixture was allowed to settle, with the upper liquid phase

containing the hydrolyzed soluble UBW. The liquid phase was recovered and circulated at 40 L h^{-1} flow rate through the UF membrane, operating with tangential flow at 7 bar inlet and 4.5 bar outlet pressure. This step yielded a retentate with 5-10 % dry matter content, which was finally dried at 60 °C. The solid CVT230 was obtained in 15-30 % w/w yield with respect to the starting UBW dry matter, and it was characterized according to a previously reported procedure [10]. Before use, CVT230 was taken up with Milli-Q^{TM} water under sonication, centrifuged and filtered through a cellulose acetate filter with 0.45 μm pore diameter (Millipore), to remove any residual insoluble matter.

To obtain the CVT230$_{sol}$ fraction, CVT230 aqueous solutions were acidified under stirring with HClO$_4$ and centrifuged (3500 rpm for 30 minutes). The supernatant solutions were then filtered through a cellulose acetate filter (0.45 μm pore diameter, Millipore). When needed, the solution pH was adjusted to 8.0 by dropwise addition of NaOH.

2.2 Irradiation tests

Photolysis of CVT230 (total volume 0.500 L, 500 mg L^{-1}) and (when relevant) of CVT230$_{sol}$ was carried out at the naturally occurring CVT230 solution pH (equal to 9.6), in a cylindrical photochemical reactor (Helios-Italquartz, Milan), equipped with a 125 W medium pressure Hg lamp (the reactor schematic representation and the lamp emission spectrum are reported in the Supporting Information, Figure 1S). The system was kept under continuous stirring; cold water circulating in the quartz jacket surrounding the lamp kept the temperature within the reactor at 25°C. The reaction was monitored at different irradiation times by measuring the following parameters on both CVT230 and CVT230$_{sol}$ (this latter irradiated as such from the beginning or, more often, extracted from CVT230 after irradiation): absorbance spectra, Excitation-Emission fluorescence Matrix (EEM), Total Organic Carbon (TOC), Dynamic Light Scattering (DLS), and surface tension. Potentiometric titrations were also performed on CVT230$_{sol}$ before and after irradiation.

Details regarding the instrumentation and analytical procedures are provided in the Analytical Procedures section of the Supporting Information.

3. Results and discussion

3.1 UV-Vis spectral analysis

Figures 1 reports the UV-Vis spectra recorded for CVT230 (500 mg L^{-1}) and the corresponding CVT230$_{sol}$ fraction, isolated at different irradiation times. Note that in this case CVT230$_{sol}$ was

4

isolated after irradiation. Different behaviors can be observed. The absorption of CVT230 decreased slowly but progressively, whereas the absorption of CVT230$_{sol}$ progressively increased. This finding is consistent with the hypothesis that one of the degradation pathways of CVT230 would be its transformation into CVT230$_{sol}$.

Figure 1. Time trends of the absorption spectra of (a) irradiated CVT230 and (b) CVT230$_{sol}$ isolated from CVT230, as a function of irradiation time. CVT230 initial concentration was 500 mg L^{-1}. Before recording the spectra the CVT230 solutions were diluted 20 times with ultrapure water.
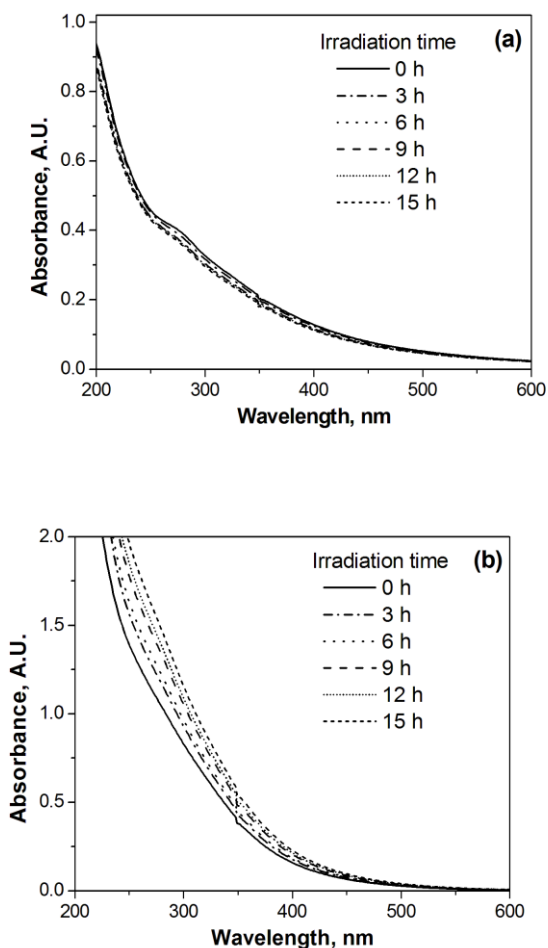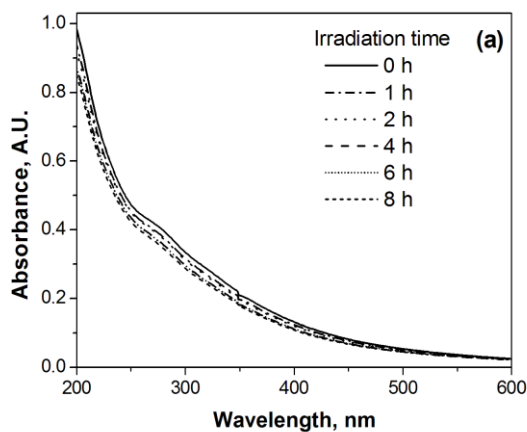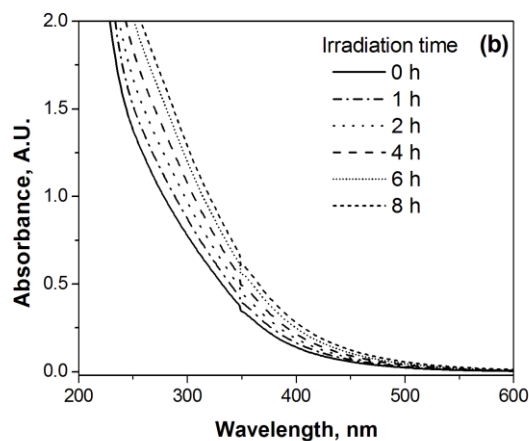
Figure 2. Time trends of the absorption spectra of irradiated (a) CVT230 and (b) CVT230$_{sol}$ isolated from CVT230, as a function of irradiation time, with 5×10^{-3} M H_2O_2 addition. CVT230 initial concentration was 500 mg L^{-1}. Before recording the spectra the CVT230 solutions were diluted 20 times with ultrapure water.

The phenomenon of the decrease of the absorbance with increasing irradiation time (Figure 1a) is often observed with surface-water chromophoric dissolved organic matter (CDOM) as well, and it is termed photobleaching [12]. Interestingly, in the present case, photobleaching was more marked if H_2O_2 was added to the SBO samples before irradiation (Figure 2a): the most likely reason is the production of $^\bullet OH$ upon H_2O_2 photolysis or Fenton-like reactions, due to the presence of a certain amount of Fe in the CVT230 composition [10]. At the alkaline pH of the irradiation experiments, the efficiency of the Fenton reaction would be low and the metal ions would mainly be involved in H_2O_2 decomposition with limited $^\bullet OH$ production [13]. However, a significant photo-Fenton activity has been reported even at circumneutral/slightly basic pH, in the presence of strong ligands such as some DOM moieties. In these conditions it was suggested an active role of iron species with high oxidation states (e.g. FeO^{2+}, ferryl ion) rather than $^\bullet OH$ [8,14].

The UV-Vis spectral analysis has been proposed previously in the literature as a tool to assess the different transformation mechanisms that may be operational during DOM photodegradation. In particular, the quotient E_2/E_3 (ratio between the absorbance at 254 and at 365 nm) has been previously found to inversely correlate with the molecular size and aromaticity of aquatic humic solutes [15]. Therefore, when E_2/E_3 increases, the aromaticity and molecular size of aquatic humic solutes is expected to decrease, and vice versa. Intra- and inter-molecular charge transfer (CT) processes between electron-donating groups (e.g., phenols) and electron-accepting groups (e.g., aromatic ketones and quinones) could yield broad absorbance above approximately 300 nm [16]. The increase in the E_2/E_3 coefficient, as a consequence of the decrease of the absorbance at 365 nm (E_3 value), could thus indicate a preferential degradation of long-wavelength absorbing

6

chromophores through destruction of CT complexes, also implying a decrease of DOM molecular weight [16,17].

Figure 3 shows the E_2/E_3 coefficient evolution with irradiation time of both CVT230 and CVT230$_{sol}$ in the presence and in the absence of H_2O_2.
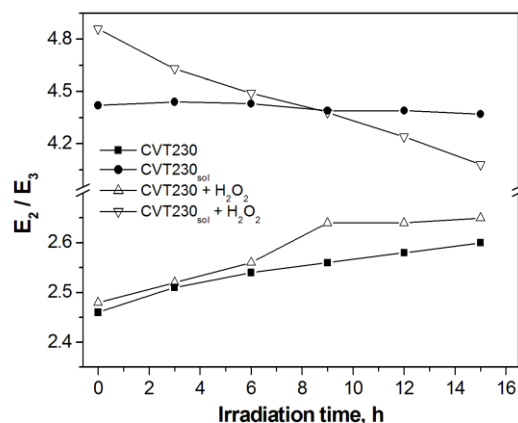

Figure 3. E_2/E_3 coefficient determined at different irradiation times for CVT230 and CVT230$_{sol}$ in the presence and in the absence of 5×10^{-3} M H_2O_2.

It can be noticed that the E_2/E_3 initial values of CVT230$_{sol}$ were almost twice as high as those of CVT230, thus suggesting that CVT230$_{sol}$ had presumably smaller size and lower aromaticity. Figure 3 also shows that, in contrast to CVT230, the E_2/E_3 values of CVT230$_{sol}$ decreased with irradiation in the presence of H_2O_2, while the corresponding values in the absence of hydrogen peroxide did not change significantly. This issue may suggest an increasing molecular weight of CVT230$_{sol}$ as long as irradiation progressed. A rationale for this finding will be proposed later on.

An alternative approach to better characterize organic matter and its photoinduced evolution is represented by the measurement of the spectral slope S before and after irradiation. Similarly to E_2/E_3, S is inversely correlated with molecular weight and aromaticity [15]. To calculate S, the absorption spectra in the 300-600 nm wavelength interval were fitted with exponential equations of the form:

$$A_1(\lambda) = A_o \, e^{-S \cdot \lambda}$$

where $A_1(\lambda)$ is the sample absorbance measured over an optical path length of 1 cm, while S and A_0 are the fitting parameters. The error on S, reported at the sigma level, depends on the scattering of the absorbance data around the exponential fit function.

The S data reported in Figure 4 suggest that: (i) irradiation increased the S values of CVT230, which could imply a decrease of molecular weight that would be consistent with the formation of

7

smaller and water-soluble species, and (ii) S was considerably higher for the soluble fraction (CVT230$_{sol}$) compared to the whole material, suggesting that CVT230$_{sol}$ had lower molecular weight than CVT230. Both results are in complete agreement with the trends observed for the E$_2$/E$_3$ quotient.

Another interesting issue, which is shown in Figure 4(b), is that the S values of CVT230$_{sol}$ decreased with irradiation time in the presence of H$_2$O$_2$, as already observed with E$_2$/E$_3$. Similarly to E$_2$/E$_3$, the S values of CVT230$_{sol}$ almost did not change with irradiation in the absence of H$_2$O$_2$. The decrease of S observed with CVT230$_{sol}$ in the presence of H$_2$O$_2$, which is at variance with the behavior of CVT230 under irradiation, would be connected to an increase of substrate molecular weight and/or aromaticity. This issue could be accounted for by either (i) photoinduced oligomerisation of the irradiated soluble material, or (ii) release of larger soluble fractions from the whole CVT230 as far as irradiation progressed. The latter hypothesis could be motivated by the fact that reaction with photogenerated $^{\bullet}$OH (the formation of which would be favored in the presence of H$_2$O$_2$) would hydroxylate the starting material, thus making it more hydrophilic [18]. Therefore, progressively larger species could become water soluble and would account for the observed increase of the molecular weight/aromaticity of the CVT230$_{sol}$ fraction. Furthermore, release of fragments from CVT230 would also result in an increase of the CVT230$_{sol}$, and eventually, of its molecular weight.
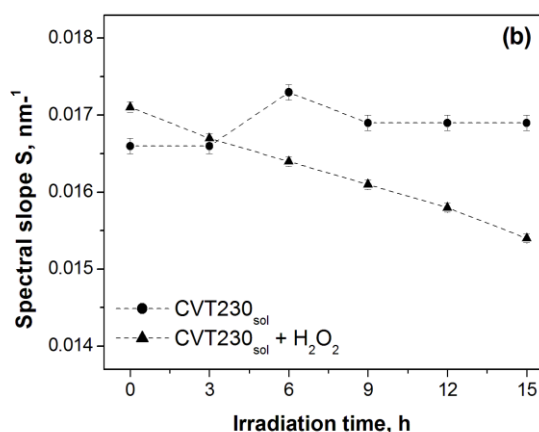

8
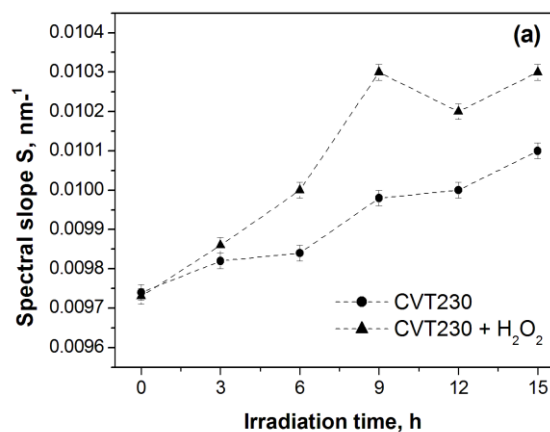
Figure 4. Time trend of the spectral slopes S, upon irradiation of the CVT230, (a): whole fraction; (b): soluble fraction, with and without H_2O_2 addition.

It should be underlined that the behavior described above was relevant to the $CVT230_{sol}$ fraction, separated from CVT230 after irradiation of the whole material. To get additional insight into the reason of the observed spectral variations in $CVT230_{sol}$, the soluble fraction was separated from CVT230 before irradiation and it was then irradiated in the absence and in the presence of H_2O_2. Figure 5 shows the time trend of the relevant absorption spectra. Photobleaching was operational in both cases, but most notably in the presence of H_2O_2. This finding confirms that the increase of $CVT230_{sol}$ absorbance with time upon irradiation of CVT230 (reported in Figures 1b and 2b) was mostly due to the photoinduced production of $CVT230_{sol}$ from CVT230. In contrast, as shown in Figure 5, $CVT230_{sol}$ present at any given time would undergo photobleaching. The trend shown for $CVT230_{sol}$ in Figure 1b (increase of absorbance upon irradiation of CVT230) suggests that the photobleached $CVT230_{sol}$ fraction was more than compensated for by newly produced $CVT230_{sol}$.
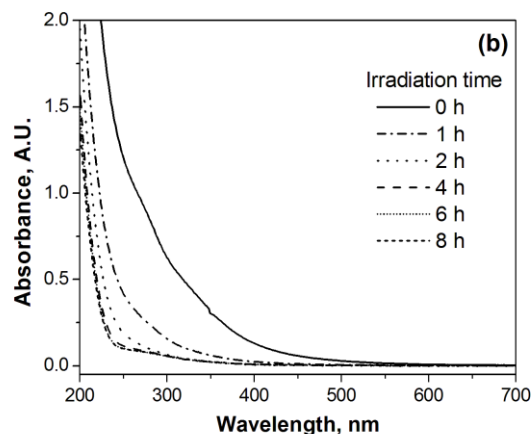

9
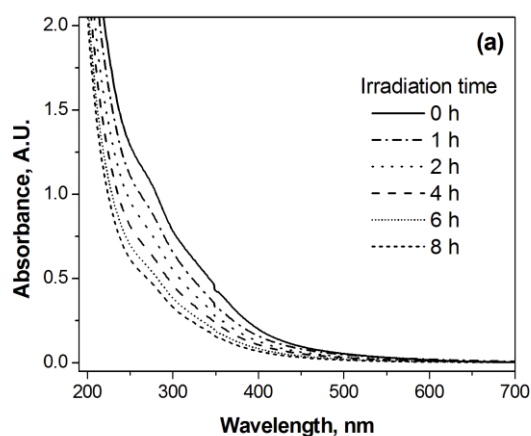
Figure 5. Time trends of the absorption spectra of CVT230$_{sol}$, as a function of the irradiation time, (a) without and (b) with H$_2$O$_2$ addition. CVT230$_{sol}$ was separated before irradiation from a 500 mg L^{-1} CVT230 solution.

Figure 6 reports the time trend of the spectral slope S, under conditions relevant to Figure 5(a) (irradiation of CVT230$_{sol}$, separated before irradiation, without H$_2$O$_2$). The plot shows that the spectral slope increased upon irradiation, which suggests a decrease of molecular weight and/or aromaticity. The photoinduced fragmentation of CVT230$_{sol}$ would be accounted for by direct photolysis, reactions of excited triplet states [19] and, possibly to a minor extent, with $^\bullet$OH that is produced to some extent by SBO materials under irradiation [7].

The trend reported in Figure 6 is consistent with the behavior of S upon irradiation of CVT230 (see Figure 4(a)), but it is in contrast with the very limited variation of S for CVT230$_{sol}$ separated after irradiation (Figure 4(b)). In the latter case, the likely decrease of the molecular weight/aromaticity of CVT230$_{sol}$ that was initially present was probably compensated for the release of larger/more aromatic soluble components as irradiation progressed.
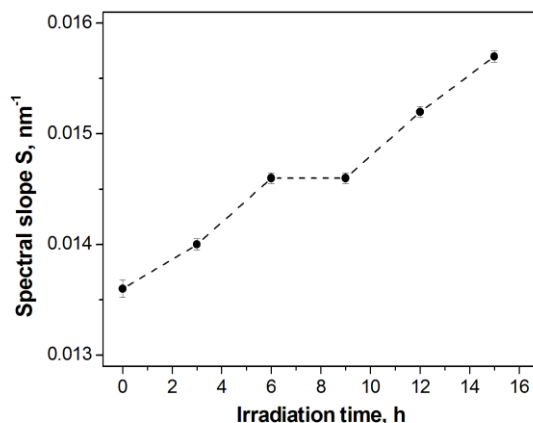

10

Figure 6. Time trend of the spectral slope S upon irradiation of CVT230$_{sol}$ (isolated from CVT230 before irradiation) without H$_2$O$_2$.

In the case of the irradiation of the pre-isolated CVT230$_{sol}$ with H$_2$O$_2$, the considerable photobleaching (Figure 5b) prevented a significant trend of S to be obtained.

3.2 Fluorescence excitation-emission matrix analysis

Fluorescence excitation-emission matrices (EEMs) were measured at different irradiation times, for both CVT230 and CVT230$_{sol}$ separated after irradiation. Figure 7 reports the EEMs for CVT230 and CVT230$_{sol}$ before irradiation and after 14 h irradiation. The results suggest a similarity in EEM contours for both CVT230 and CVT230$_{sol}$, which were characterized by one peak at excitation/emission (Ex/Em) wavelengths (nm) of 320/430 for CVT230 and 330/420 for CVT230$_{sol}$. Several works reported in the literature, commonly assigned these peaks to the presence of humic acid-like substances [20-22]. With increasing irradiation time the fluorescence intensity of CVT230 decreased gradually, which is consistent with the photodegradation of its fluorophore groups. A similar behavior has also been observed for the photo-oxidation of commercial humic acids [23]. On the contrary, in the case of CVT230$_{sol}$ the fluorescence intensity at 330/420 Ex/Em remained almost constant after 14 h of irradiation.
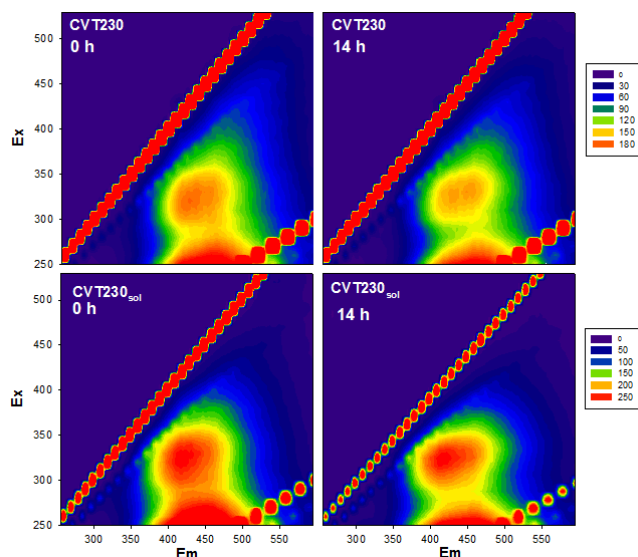

Figure 7. EEM of CVT230 and CVT230$_{sol}$ measured for CVT230 at different irradiation times.

To get further insight into the fluorophores of both CVT230 and CVT230$_{sol}$, the entire set of the EEM data at various irradiation times was examined using Parallel Factor Analysis (PARAFAC; see Supporting Information for a detailed description of the model approach).

11

All the fluorescence EEMs of CVT230 could be successfully decomposed by PARAFAC analysis into a three-component model. The fluorescence intensities of these components (C1, C2 and C3) are shown in Figure 8. Their excitation/emission coordinates are equal to 345/470 nm (C1), 310/410 nm (C2) and 280/520-450/520 nm (C3). C1 could be associated with humic-like substances from terrestrial organic matter because it is similar to the PARAFAC components found by Fellman et al. [24], Yang et al. [25] and Stedmont et al. [26]. The second component, C2, is considered as a humic-like fraction of organic matter from microbial production [27]. C3 has excitation and emission maxima similar to semi-quinone-like fluorophores [28] and it is expected to consist of hydrophobic compounds with large molecular size [29]. The PARAFAC deconvolution also indicated a decrease with irradiation time of the fluorescence intensity of each component (Figure 9(a)). In particular, the component most sensitive to photodegradation was C3, in agreement with the results reported by Ishii and Boyer [29].
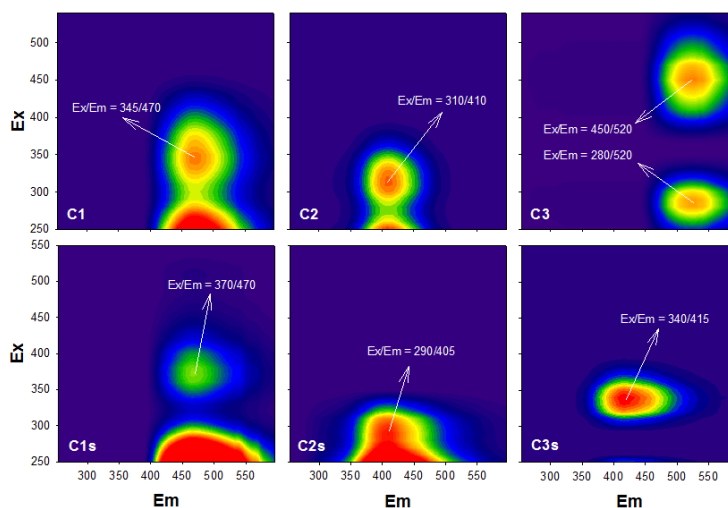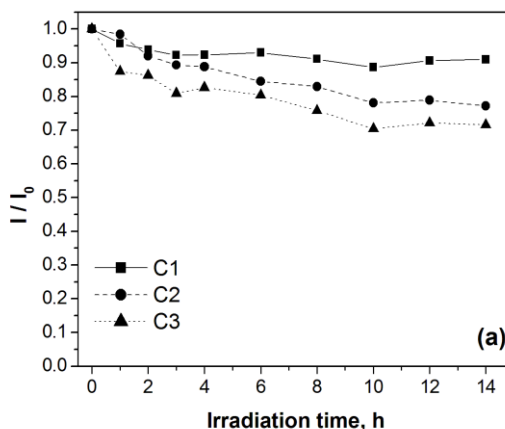

Figure 8. EEMs contours of the three components identified by the PARAFAC model for CVT230 (C1, C2 and C3) and for CVT230$_{sol}$ (C1s, C2s, C3s).
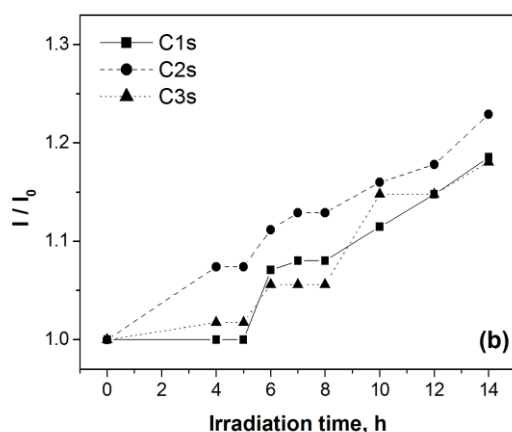
Figure 9. Changes in the fluorescence intensity of three PARAFAC-derived components with the irradiation time for (a) CVT230 and (b) CVT230$_{sol}$.

PARAFAC analysis was also performed on the EEMs data of CVT230$_{sol}$ at different irradiation times. Again, as in the case of CVT230, a three-component model was obtained, although with a different position of the fluorescence maxima compared to CVT230 (Figure 8). In this case, two components, C1s (370/470) and C2s (290/405), are similar to humic-like substances [24,26] and the third component, C3s (340/415), could be related to the hydrophilic fraction of humic-like substances identified by Chen et al. [20]. The absence of the component C3 (large molecular size and hydrophobic compounds) in CVT230$_{sol}$ is in agreement with the lower molecular size found for CVT230$_{sol}$ (UV-Vis data) and with the presence of a more water soluble material. The analysis of the fluorescence intensities of each component with irradiation time shows an overall increase (Figure 9(b)). This behavior is consistent with the observed UV-Vis spectra of CVT230$_{sol}$, and it makes further evidence of the increase of the soluble fraction as irradiation progressed.

3.3 Organic carbon evolution and mineralization

The TOC values of the 500 mg L^{-1} solutions before irradiation showed that CVT230 contained about 35% of carbon in weight, and about one fourth of the carbon content was accounted for the soluble fraction (CVT230$_{sol}$). Figure 10 shows the TOC evolution of CVT230 and CVT230$_{sol}$ at different irradiation times. After 14 h of irradiation, CVT230 still retained around 90% of its initial carbon, implying that mineralization was limited to about one tenth of the total material. Interestingly, of the 90% non-mineralized carbon of irradiated CVT230, almost two-thirds belonged to the soluble CVT230$_{sol}$ fraction, to be compared with the one fourth carbon share of CVT230$_{sol}$ before irradiation. Indeed, the carbon concentration of CVT230$_{sol}$ increased with irradiation from 42.5 mg L^{-1} up to 99.9 mg L^{-1}. This result is consistent with the absorbance data reported in Figures

13

1 and 2 and with the fluorescence data of Figures 7 and 8, and it clearly indicates that the degradation of CVT230 produced soluble compounds.
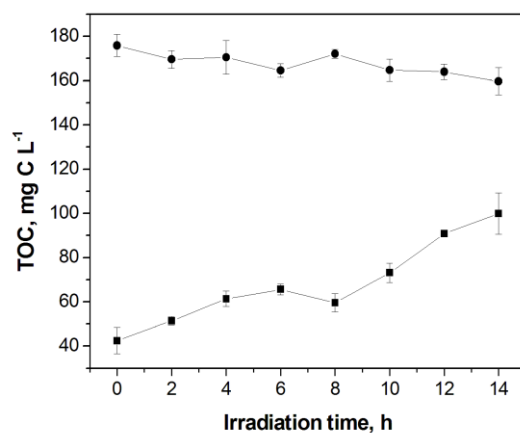

Figure 10. TOC evolution of CVT230 (●) and CVT230$_{sol}$ (■) as a function of the irradiation time.

Interestingly, the photoinduced increase of the absorbance of CVT230$_{sol}$ (extracted from CVT230 after irradiation) was less marked than the TOC increase, as shown by the trend of the CVT230$_{sol}$ specific absorbance (A$_{254}$/TOC, namely the ratio between the absorbance at 254 nm and the TOC value) (Figure 3S in the Supporting Information). This issue could be consistent with the fact that the soluble material released at any given time would undergo considerable photobleaching under irradiation (Figure 5) but limited mineralization (Figure 10). Moreover, the decrease of A$_{254}$/TOC with time suggests a decrement in the aromaticity of the soluble fraction upon irradiation [23].

3.4 Dimensional characterization

Dynamic light scattering (DLS) measurements were carried out on CVT230 and CVT230$_{sol}$ samples taken at different irradiation times (with CVT230$_{sol}$ separated from CVT230 after irradiation). The trend of the hydrodynamic radii (r$_{hyd}$) estimated from DLS measurements is shown in Figure 11. It can be seen that the r$_{hyd}$ of CVT230 remained almost constant with irradiation, close to a value of 135 nm. In contrast, a slow but non negligible increasing trend could be observed for CVT230$_{sol}$. Moreover, the initial r$_{hyd}$ value was lower for CVT230$_{sol}$ (about 100 nm), in agreement with the previously hypothesized lower size of the molecular aggregates of the soluble fraction.

Note that the DLS technique is silent about the nature of the scattered particles, as it only measures the hydrodynamic radii of their aggregates. The results shown in Figure 11 suggest that the size of the CVT230 scattering centers is not highly affected by irradiation, although a decrement in the molecular weight is well supported by the spectroscopic data reported previously. It could be

14

possible that although there is a decrease in the weight of the individual molecules (as shown by the E2/E3 and S) there is no decrease in the size of the aggregates of molecules.

Interestingly, CVT230 has very similar hydrodynamic radii compared to commercial Aldrich humic acid (130 vs. 135 nm, respectively) [30].

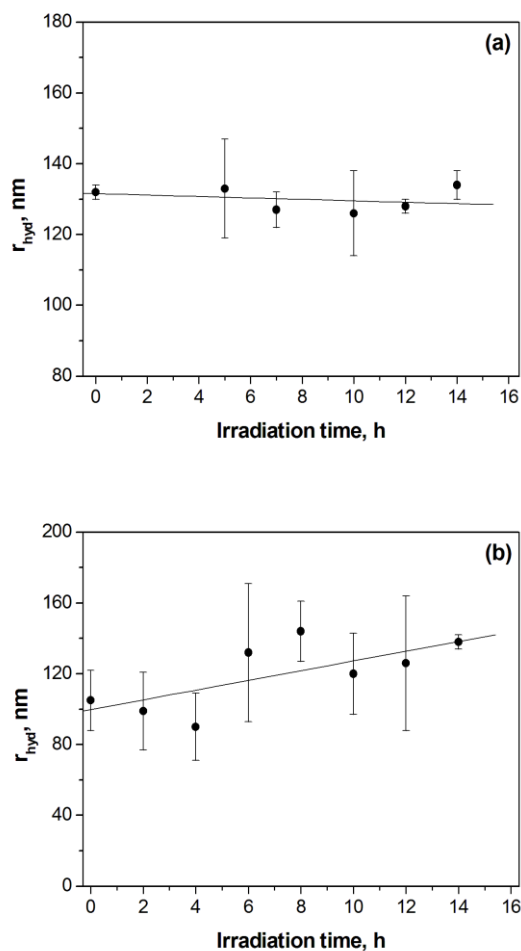**Figure 11**. Effect of irradiation on the r_{hyd} of CVT230 (a) and of CVT230$_{sol}$ (b) solution. The error bounds represent the confidential interval obtained for at least three independent measurements at 95% confidence.

3.5 Acidic groups titration

Potentiometric titration was used to identify and quantify the acidic functions of CVT230 and CVT230$_{sol}$, before and after irradiation.

15

The experimental curves were elaborated in order to attain a chemical model that accounts for the acid-base behavior of the studied material. With the software BSTAC [31] it was possible to calculate the concentration of protogenic sites and the relative protonation constants (see Table 1S in the Supporting Information).

The literature dealing with the protonation of humic substances assumes that the total concentrations of carboxylic (COOH) and phenolic (PhOH) functional groups can be obtained as the sum of the concentration values for the species with $\log\beta < 8$ (assimilated as COOH) and with $\log\beta > 8$ (PhOH). [32] In the present case, because CVT230 also has amines and other nitrogen functions, the attribution of $\log\beta$ values to a specific functional group is not allowed. However, it is reasonable to suppose that the sites having $\log\beta < 7$ can be assigned to –COOH groups. The total concentration of –COOH obtained from the chemical model, calculated as the sum of the concentrations of the species with $\log\beta < 7$, was affected by the degradation process only in the case of CVT230$_{sol}$. Here the –COOH concentrations were 0.66 ± 0.05 and 2.1 ± 0.7 mmol L^{-1}, respectively before and after 15 hours of irradiation of a 500 mg L^{-1} solution of CVT230. Therefore, the acidity of the soluble fraction increased upon irradiation. Moreover, if the concentration values are expressed in relation to the content of organic carbon, the –COOH concentrations of CVT230$_{sol}$ would be 15 ± 1 and 21 ± 8 mmol g$_C^{-1}$ before and after irradiation, respectively. These two values are coincident within the experimental error and they allow the hypothesis that the increase in the carbon content of the soluble fraction after irradiation could mainly be due to the increase of the carboxylic functions. This finding is in agreement with previous results, because it suggests that irradiation could produce increasingly larger soluble components by favoring the formation of water-soluble groups (-COOH functions). Additionally, it was shown by FTIR spectroscopy that irradiation with $\lambda > 320$ nm of a humic acid-rich soil extract resulted in a drastic decrease of the 1385 cm^{-1} absorption band [33] assigned to Fe(III)-carbozylate complexes [34]. Thus, the decrease of the carboxylate fraction complexed with Fe(III) could account for the increase of the titratable carboxylic groups.

Considering that carboxylic acids are frequently employed in the solar photo-Fenton treatment of wastewater, [35] the above data suggest that irradiation would not negatively influence the capability of SBO$_{sol}$ to promote Fenton like processes. However, further investigation is needed over this topic.

The increased concentration of hydrophilic carboxylic functions reflects also on the surfactant properties of CVT230 (see Figure 4S in the Supplementary Information).

16

It can be observed that the surface tension of CVT230 solution increases progressively when increasing the irradiation time, until a value close to the one corresponding to the pure water is attained (about 70.5 mN m^{-1}), thus evidencing that CVT230 surfactant properties are lost. This behavior may be due to the production of more hydrophilic species that decrease the amphiphilic features of CVT230 and, consequently, its surfactant characteristics.

4. Conclusions

The irradiation of CVT230, chosen as model SBO, induced several changes, which can be summarized as follows:

1) The irradiated material progressively became more hydrophilic, with an increasing number of carboxylic groups and a decrease (till complete loss) of its surfactant properties. The formation of hydrophilic species accounted for the progressive increase of the SBO acid-soluble fraction.

2) Photobleaching of the whole SBO was also observed, which suggests the degradation of the chromophores. The fluorophores were photodegraded as well, as indicated by the decrease of the fluorescence intensity.

3) Irradiation decreased the size of whole SBO, but there is evidence of an increase in the average size of the molecular aggregates of the soluble fraction. The latter could be accounted for by the photoinduced formation of increasingly more hydrophilic species, which would allow progressively larger components to become soluble.

5. Acknowledgements

6. References

[1] E. Montoneri, D. Mainero, V. Boffa, D.G. Perrone, C. Montoneri, Biochemenergy: a project to turn a urban wastes treatment plant into biorefinery for the production of energy, chemicals and consumer's products with friendly enviromental impact, Int. J. Global Environ. 11 (2011) 170-196.
[2] www.biochemenergy.it (last accessed January, 2015).

[3] A. Amine-Khodja, O. Trubetskaya, O. Trubetskoj, L. Cavani, C. Ciavatta, G. Guyot, C. Richard, Humic-like substances extracted from composts can promote the photodegradation of Irgarol 1051 in solar light, Chemosphere 62 (2006) 1021-1027.

[4] S. Canonica, U. Jans, K. Stemmler, J. Hoigné, Transformation kinetics of phenols in water: photosensitization by dissolved natural organic material and aromatic ketones, Environ. Sci. Technol. 29 (1995) 1822-1831.

[5] J. Wenk, U. Von Gunten, S. Canonica, Effect of dissolved organic matter on the transformation of contaminants induced by excited triplet states and the hydroxyl radical, Environ. Sci. Technol. 45 (2011) 1334-1340.

[6] S. E. Page, W. A. Arnold, K. McNeill, Assessing the contribution of free hydroxyl radical in organic matter-sensitized photohydroxylation reactions, Environ. Sci. Technol. 45 (2011) 2818-2825.

[7] P. Avetta, F. Bella, A. Bianco Prevot, E. Laurenti, E. Montoneri, A. Arques, L. Carlos, Waste Cleaning Waste: photodegradation of monochlorophenols in the presence of waste-derived photosensitizer, ACS Sustain. Chem. Eng. 1 (2013) 1545−1550.

[8] J. Gomis, R.F. Vercher, A.M. Amat, D.O. Mártire, M.C. González, A. Bianco Prevot, E. Montoneri, A. Arques, L. Carlos, Application of soluble bio-organic substances (SBO) as photocatalysts for wastewater treatment: sensitizing effect and photo-Fenton-like process, Catal. Today 209 (2013) 176–180.

[9]P. Avetta, A. Bianco Prevot, D. Fabbri, E. Montoneri, L. Tomasso, Photodegradation of naphthalene sulfonic compounds in the presence of a bio-waste derived sensitizer, Chem. Eng. J. 197 (2012) 193–198.

[10] E. Montoneri, V. Boffa, P. Savarino, D. G. Perrone, M. Ghezzo, C. Montoneri, R. Mendichi, Acid soluble bio-organic substances isolated from urban bio-waste. Chemical composition and properties of products, Waste Manage. 31 (2011) 10–17.

[11] J. Gomis, A. Bianco Prevot, E. Montoneri, M.C. Gonzalez, A.M. Amat, D.O. Martire, A. Arques, L. Carlos, Waste sourced bio-based substances for solar-driven wastewater remediation: Photodegradation of emerging pollutants, Chem. Eng. J. 235 (2014) 236-243.

[12] B. Sulzberger, E. Durisch-Kaiser, Chemical characterization of dissolved organic matter (DOM): A prerequisite for understanding UV-induced changes of DOM absorption properties and bioavailability, Aquat. Sci. 71 (2009) 104-126.

[13] A.W. Vermilyea, B.M. Voelker, Photo-Fenton reaction at near-neutral pH, Environ. Sci. Technol. 43 (2009) 6927-6933.

[14] H. Bataineh, O. Pestovsky, A. Bakac, pH-induced mechanistic changeover from hydroxyl radicals to iron(IV) in the Fenton reaction, Chem. Sci. 3 (2012) 1594-1599.

[15] J. Peuravuori, K. Pihlaja, Molecular size distribution and spectroscopic properties of aquatic humic substances, Anal. Chim. Acta 337 (1997) 133-149.

[16] C.M. Sharpless, N.V. Blough, The importance of charge-transfer interactions in determining chromophoric dissolved organic matter (CDOM) optical and photochemical properties, Environ. Sci.: Processes Impacts 16 (2014) 654-671.

[17] M. Lipski, J. Stawinski, D. Zych Changes, Changes in The Luminescent Properties of Humic Acids Induced by UV Radiation, J. Fluoresc. 9 (1999) 133-138.

[18] O. Legrini, E. Oliveros, A.M. Braun, Photochemical processes for water treatment, Chem. Rev. 93 (1993) 671-698.

[19] S. Canonica, Oxidation of aquatic organic contaminants induced by excited triplet states, Chimia 61 (2007) 641-644.

[20] W. Chen, P. Westerhoff, J.A. Leenheer, K. Booksh, Fluorescence Excitation−Emission Matrix Regional Integration to Quantify Spectra for Dissolved Organic Matter, Environ. Sci. Technol. 37 (2003) 5701-5710.

[21] P.G. Coble, Characterization of marine and terrestrial DOM in seawater using excitation-emission matrix spectroscopy, Mar. Chem. 51 (1996) 325-346.

[22] E. De Laurentiis, M. Minella, V. Maurino, C. Minero, M. Brigante, G. Mailhot, D. Vione, Photochemical production of organic matter triplet states in water samples from mountain lakes, located below or above the tree line, Chemosphere 88 (2012) 1208-1213.

[23] S. Sen Kavurmaci, M. Bekbolet, Tracing TiO_2 photocatalytic degradation of humic acid in the presenceof clay particles by excitation–emission matrix (EEM) fluorescence spectra, J. Photoch. Photobio. A 282 (2014) 53–61.

[24] J.B. Fellman, M.P. Miller, R.M. Cory, D.V. D'Amore, D. White, Characterizing dissolved organic matter using PARAFAC modeling of fluorescence spectroscopy: A comparison of two models, Environ. Sci. Technol. 43 (2009) 6228-6234.

[25] X. Yang, F. Meng, G. Huang, L. Sun, Z. Lin, Sunlight-induced changes in chromophores and fluorophores of wastewater-derived organic matter in receiving waters - The role of salinity, Water Res. 62 (2014) 281-292.

[26] C.A. Stedmon, S. Markager, R. Bro, Tracing dissolved organic matter in aquatic environments using a new approach to fluorescence spectroscopy, Mar. Chem. 82 (2003) 239-254.

[27] B.A. Lyon, R.M. Cory, H.S. Weinberg, Changes in dissolved organic matter fluorescence and disinfection byproduct formation from UV and subsequent chlorination/chloramination, J. Hazard. Mater. 264 (2014) 411-419.

[28] R.M. Cory, D.M. McKnight, Fluorescence spectroscopy reveals ubiquitous presence of oxidized and reduced quinones in dissolved organic matter, Environ. Sci. Technol. 39 (2005) 8142-8149.

[29] S.K. Ishii, T.H. Boyer, Behavior of Reoccurring PARAFAC Components in Fluorescent Dissolved Organic Matter in Natural and Engineered Systems: A Critical Review, Environ. Sci. Technol. 46 (2012) 2006-2017.

[30] M. Minella, M.P. Merlo, V. Maurino, C. Minero, D. Vione, Transformation of 2,4,6-trimethylphenol and furfuryl alcohol, photosensitized by Aldrich humic acids subject to different filtration procedures, Chemosphere 90 (2013) 306–311.

[31] C. De Stefano, P. Mineo, C. Rigano, S. Sammartano, Ionic-strength dependence of formation-constants. The calculation of equilibrium concentrations and formation-constants, Ann. Chim. 83 (1993) 243-277.

[32] E.B.H Santos, V.I. Esteves, J.P.C. Rodrigues, A.C. Duarte, Humic substances' proton-binding equilibria: Assessment of errors and limitations of potentiometric data, Anal. Chim. Acta 392 (1999) 333-341.

[33] G.N. Bosio, P.D. Gara, F.S.G Einschlag, M.C. Gonzalez, M.T. Del Panno, D.O. Martire, Photodegradation of soil organic matter and its effect on gram-negative bacterial growth, Photochem. Photobiol. 84 (2008) 1126-1132.

[34] X.X. Ou, S. Chen, X. Quan, H.M. Zhao, Photochemical activity and characterization of the complex of humic acids with iron(III), J. Geochem. Explor. 102 (2009) 49-55.

[35] J.H.O.S. Pereira, D.B. Queiros, A.C. Reis, O.C. Nunes, M.T. Borges, R.A. Boaventura, V.J.P. Vilara, Process enhancement at near neutral pH of a homogeneous photo-Fenton reaction using ferricarboxylate complexes: Application to oxytetracycline degradation, Chem. Eng. J. 253 (2014) 217-228.